Carbohydrate Polymers 82 (2010) 21–27

Contents lists available at ScienceDirect

Carbohydrate Polymers

journal homepage: www.elsevier.com/locate/carbpol

Preparation and cell culture behavior of self-assembled monolayers composed of chitohexaose and chitosan hexamer

Yuka Yoshiike, Shingo Yokota, Nobuo Tanaka, Takuya Kitaoka*, Hiroyuki Wariishi

Department of Forest and Forest Products Sciences, Graduate School of Bioresource and Bioenvironmental Sciences, Kyushu University, 6-10-1 Hakozaki, Higashi-ku, Fukuoka 812-8581, Japan

ARTICLE INFO

Article history:
Received 24 February 2010
Received in revised form 5 April 2010
Accepted 7 April 2010
Available online 14 April 2010

Keywords:
Chitin
Chitosan
Self-assembled monolayer
Sugar density
Cell culture
Glyco-scaffold

ABSTRACT

Chitohexaose and chitosan hexamer were site-selectively modified at each reducing end with thiosemicarbazide, followed by self-assembly chemisorption of the S-derivatives on a gold substrate *via* S–Au bonding. Quartz crystal microbalance analysis and X-ray photoelectron spectroscopy suggested successful formation of self-assembled monolayers (SAMs) consisting of chitin and chitosan with sugar densities 0.39 and 0.35 chains nm^{-2}, respectively. As-prepared SAMs were very hydrophilic (with water contact angles 12–13°) and flat at the nanometer scale (RMS ≈ 1.7 nm). Mouse fibroblasts (NIH-3T3) preferentially adhered to both SAMs, while fewer cells were attached to the more hydrophobic, intact gold substrate. The fixed carbohydrates induced good proliferation of NIH-3T3 cells, while surface treatment with free sugars had almost no positive effects. This architectural design of water-soluble oligosaccharide-SAMs is expected to provide a new approach for functional development of carbohydrate-decorated biointerfaces.

1. Introduction

Carbohydrates are closely involved in a wide variety of biological processes such as cell–cell communications, immunological responses and other physiological phenomena (Boyan, Hummert, Dean, & Schwartz, 1996; Lim, Liu, Vogler, & Donahue, 2004; Park et al., 2003). Structural and bio-functional design of glyco-scaffolds for tissue culture, aimed at carbohydrate-mediated interactions, has recently attracted a great deal of attention in cell engineering fields (Barbucci et al., 2005; Mori, Sekine, Hasegawa, & Okahata, 2007; Onodera et al., 2006). In particular, fabrication and immobilization methods for bio-functional carbohydrates have become of great importance for practical applications. For example, it has been reported that hyaluronan (HA), one of the most important extracellular matrices, was grafted to silicon oxide surface through conjugation to (3-amino-propyl)trimethoxysilane with the carboxylate groups of HA (Pasqui, Atrei, & Barbucci, 2007). Carboxymethylcellulose (CMC) hydrogel has been enzymatically prepared through horseradish peroxidase-catalyzed oxidative crosslinking of phenolic OH groups introduced into CMC chains (Ogushi, Sakai, & Kawakami, 2009). Although many strategies have been developed for design of carbohydrate-based scaffolds, these approaches have typically involved immoderate chemical modification of polymer backbones. There have been few reports of studies in which the original molecular structure was retained, and chain alignment as well as sugar density on the scaffold surfaces were controlled for cell culture applications of carbohydrate-based materials.

Chitin, a linear polymer of β-1,4-linked *N*-acetyl-D-glucosamine (GlcNAc), is widely distributed in nature as the exoskeleton of crustaceans and insects, and as the major component of the cell walls of bacteria and fungi (Rinaudo, 2006). It is the second (after cellulose) most abundant bioresource on earth, and is estimated to be accumulated in extremely large quantities (>10^9 tons). Chitosan is a linear, cationic polysaccharide composed of β-1,4-linked D-glucosamine (GlcN), and is produced by deacetylation of chitin. Both chitin and chitosan are known to have unique biological properties, *e.g.* biocompatibility, biodegradability, non-toxicity and wound-healing effects (Morimoto, Saimoto, & Shigemasa, 2002). Moreover, their component sugars, GlcNAc and GlcN, are major bioactive sugars and play significant roles in most biological phenomena (Chen, Du, Wu, & Xiao, 2002; Xu, Mccarthy, & Gross, 1996). For these reasons chitin and chitosan have attracted much attention in biomedical fields, and many investigations of layer formation for scaffold applications in cell culture have been reported, *e.g.* spin-coated films (Ligler, Lingertfelt, Price, & Schoen, 2001), non-woven fabrics (Suzuki et al., 2008) and hydrogels (Tamura, Nagahama, & Tokura, 2006). However, these approaches require long chain polysaccharides and irreversible insolubilization for formation of stable scaffold matrices for aqueous cell culture, and encounter dif-

* Corresponding author. Tel.: +81 92 642 2993; fax: +81 92 642 2993.
E-mail address: tkitaoka@agr.kyushu-u.ac.jp (T. Kitaoka).

0144-8617/$ – see front matter © 2010 Elsevier Ltd. All rights reserved.
doi:10.1016/j.carbpol.2010.04.015

ficulties in controlling molecular orientation, surface morphology and sugar density.

In our previous studies, cellulose nanolayers with parallel chain alignment were successfully prepared *via* chemoselective modification of the reducing ends of cellulose with thiosemicarbazide (TSC), and subsequent self-assembly chemisorption on a gold (Au) surface (Yokota, Kitaoka, Sugiyama, & Wariishi, 2007). This approach utilizes S-derivatization of one terminus (reducing end) of polysaccharide and spontaneous S–Au interaction, which can be applied to a variety of polysaccharides including methylcellulose, carboxymethylcellulose and hydroxyethylcellulose (Yokota, Matsuyama, Kitaoka, & Wariishi, 2007; Yokota, Kitaoka, & Wariishi, 2008). The carbohydrate-fixed nanolayers had bio-functional characteristics for cell culture, and promoted or inhibited adhesion of rat liver cells (IAR-20) to these surfaces, depending on the sugar structures (Yokota, Kitaoka, & Wariishi, 2008). In addition, carbohydrate chains fixed on the Au substrates might be orientated to some extent because of the terminal immobilization of only reducing ends on the surfaces and the outer surfaces of as-designed nanolayers possibly involved the non-reducing end groups, which are important for interaction with various receptors on cell surfaces. This vectorial chain immobilization technique is expected to provide a new approach for functional development of chitin and chitosan-based scaffolds.

In the present study, water-soluble chitohexaose (abbreviated here as βGlcNAc6) and chitosan hexamer (βGlcN6) were site-selectively modified at each reducing end with TSC according to the methods outlined above, and self-assembled monolayers (SAMs) were prepared on an Au-coated glass plate without impairing most of the inherent molecular structures and characteristics. Self-assembly formation and surface characteristics of oligochitin-SAM (βGlcNAc6-SAM) and oligochitosan-SAM (βGlcN6-SAM) were investigated by quartz crystal microbalance (QCM) analysis, X-ray photoelectron spectroscopy (XPS) and atomic force microscopy (AFM). Both carbohydrate-SAMs were subjected to cell culture assay using mouse fibroblasts (NIH-3T3), and their bio-functional properties are discussed.

2. Experimental

2.1. Materials

Pure hexa-*N*-acetyl-chitohexaose (βGlcNAc6; with degree of polymerization (DP) = 6) and chitosan hexamer (βGlcN6; DP = 6) were purchased from Seikagaku Biobusiness Corp. (Japan). *N*-Methylmorpholine *N*-oxide (NMMO) and thiosemicarbazide (TSC) were obtained from Sigma–Aldrich Corp. (USA) and Wako Pure Chemical Ind. Ltd. (Japan), respectively. Micro cover glass (diameter: 15 mm, Matsunami Glass Ind. Ltd., Japan) was used as a flat, transparent substrate. The water used in this study was purified with a Milli-Q system (Millipore Corp., USA). Mouse fibroblasts (NIH-3T3) were provided by DS Pharma Biomedical Co. Ltd. (Japan). Dulbecco's Modified Eagle's Medium (DMEM), glutamine, penicillin–streptomycin, trypsin, and ethylenediaminetetraacetic acid (EDTA) were purchased from Invitrogen Corp. (USA). Fetal bovine serum (FBS) was obtained from Biowest Co. Ltd. (France). Tissue culture polystyrene (TCPS) dishes and plates (24-well) were obtained from Sumitomo Bakelite Co. Ltd. (Japan). Sodium cyanoborohydride ($NaCNBH_3$) and other chemicals were reagent grade and used without further purification.

2.2. Preparation of βGlcNAc6- and βGlcN6-SAMs

An outline of the preparation of βGlcNAc6- and βGlcN6-SAMs is shown in Fig. 1. Terminal TSC-functionalization of βGlcNAc6 reducing ends was carried out as previously reported (Yokota, Kitaoka, & Wariishi, 2008; Yokota, Kitaoka, Opietnik, Rosenau, & Wariishi, 2008). Powdery βGlcNAc6 was completely dissolved at a concentration of 0.4% (w/w) in an 80% NMMO/H_2O mixture at 70 °C, then the TSC reagent in amount equal to that of βGlcNAc6 was poured into the mixture, followed by stirring for 90 min. The resulting βGlcNAc6 thiosemicarbazone (βGlcNAc6-TSC, shown in Fig. 1) was obtained in 38.8% yield by precipitation with ethanol, and rinsing with additional ethanol by repeated (at least five times) centrifugation (3000 rpm, R.T.) to remove unreacted TSC residues. Subsequently, βGlcN6-TSC was prepared by aqueous reductive amination with $NaCNBH_3$. βGlcN6 powder was dissolved (20 mg mL^{-1}) in Milli-Q water, followed by reaction with the same amount (20 mg mL^{-1}) of TSC at 70 °C for 24 h in the presence of $NaCNBH_3$ (1.0 mmol mL^{-1}). As-prepared βGlcN6-TSC was precipitated with 1% NaOH aq./methanol (1/20, v/v), then centrifuged five times (3000 rpm, R.T.) to remove excess $NaCNBH_3$ and unreacted TSC, resulting in a 95.6% yield. As-prepared βGlcNAc6-TSC and βGlcN6-TSC possibly possessed respective ring-open, amine forms as shown in Fig. 1; however there is room for further improvement towards higher yield and more detailed structural identification of βGlcNAc6-TSC.

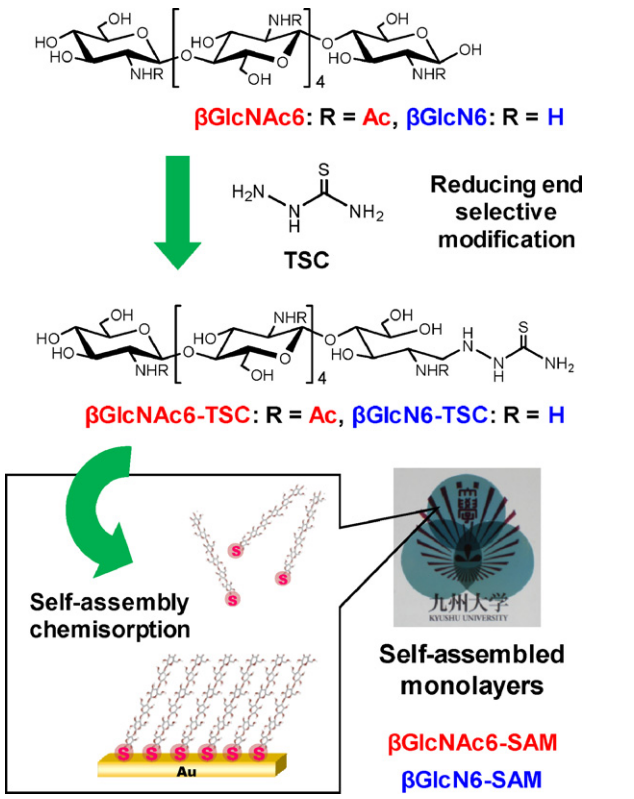

Fig. 1. Schematic illustration of TSC-derivatization and spontaneous self-assembly immobilization of βGlcNAc6 and βGlcN6. The photograph is an optical image of carbohydrate-SAMs.

Piranha-washed glass plates were coated with *ca.* 23 nm of Au by ion sputtering (VPS-020, ULVAC Inc., Japan). The Au-coated plate was soaked in 0.02% (w/v) βGlcNAc6-TSC aqueous solution at R.T. for 24 h, followed by thorough washing with Milli-Q water and ethanol, to prepare βGlcNAc6-SAM. In the case of βGlcN6-SAM, the Au plate was soaked, at R.T. for 24 h, in 0.1% (w/v) βGlcN6-TSC acidic aqueous solution adjusted to pH 4.0 with HCl, followed by sequential washing with acidic water, Milli-Q water and ethanol. As controls, the Au plates were soaked in each solution of TSC-free

carbohydrates in a similar manner. Both as-prepared carbohydrate-SAMs were dried in a flow of inert (nitrogen) gas, then sterilized *via* UV irradiation (12 h) for cell culture assay.

2.3. Characterization

A QCM apparatus (AFFINIXQ, Initium Inc., Japan) with a 27 MHz AT-cut, Au-coated quartz crystal was used to quantitatively measure the amount of carbohydrate–TSC molecules chemisorbed on the Au surface of a QCM sensor chip. An aqueous solution of each carbohydrate–TSC (0.7%, w/v, 8.0 μL) was added in one injection to a sample chamber, into which 8.0 mL of neutral Milli-Q water (pH 7.0) or acidic water (pH 4.0) had been pre-loaded. The frequency changes of the sensor chip were monitored on line at 25 °C, with stirring at 1000 rpm.

Elemental analysis of the surfaces of βGlcNAc6-SAM and βGlcN6-SAM was carried out using an AXIS-HSi XPS apparatus (Shimadzu/Kratos Co. Ltd., Japan) equipped with a monochromatic Al Kα X-ray source (1486.6 eV). XPS analysis was performed at 15 kV voltage and 10 mA current, and the analyzing chamber pressure was maintained below 0.5 μPa during the measurement. The pass energy and step width for narrow scans were set at 40 and 0.05 eV, respectively. For the survey scan those parameters were set at 80 and 1 eV. The binding energies for all spectra were referenced to a C 1s signal (reduced C–C band) at 285.0 eV.

The surface morphology of carbohydrate-SAMs was visualized by tapping mode AFM imaging. AFM observation was performed under ambient conditions using a NanoScope IIIa atomic force microscope (Veeco Instruments Inc., USA) with an E-type piezoelectric scanner and single-crystal silicon tip (Veeco Instruments Inc., USA) with length 125 μm, radius of curvature 5–10 nm, spring constant 20–100 N m^{-1}, and resonance frequency 200–400 kHz. AFM measurements were carried out in three different regions (with scan size 1.0 μm × 1.0 μm) per sample. The morphological data of captured AFM images were analyzed using the AFM-accessory software.

The contact angle of a water droplet on βGlcNAc6-SAM and βGlcN6-SAM was measured with a DropMaster 500 (Kyowa Interface Science Co. Ltd., Japan) contact angle meter using the sessile drop technique. A water drop (1.0 μL) was gently placed on the SAM at 20 °C, and digital images of the water droplet were sequentially captured at 1 s intervals and simultaneously analyzed using the analytical software supplied with the apparatus.

2.4. Cell adhesion assay

Sterilized βGlcNAc6-SAM and βGlcN6-SAM on Au-coated glass plates were placed one by one in contact with both bottom and wall of each well of 24-well TCPS plates, and medium suspensions of NIH-3T3 cells (1 mL) were seeded on each substrate (1.0×10^5 cells mL^{-1}, *i.e.* 1.0×10^5 cells per well). After incubation for 3, 6, 24 and 48 h with DMEM supplemented with 10% (v/v) FBS and 5% (v/v) penicillin–streptomycin in a 5% CO_2 atmosphere at 37 °C, unattached cells were completely removed by twice rinsing with phosphate buffered saline (PBS) solution. The adhered cells on the SAMs were then treated with trypsin–EDTA, and enzymatically detached cells were counted using a counting chamber. Microscopic images of cell adhesion and proliferation were acquired with a Leica DMI 4000B (Leica Microsystems Co. Ltd., Germany).

3. Results and discussion

3.1. Self-assembly immobilization of βGlcNAc6-TSC and βGlcN6-TSC on a gold surface

SAM formation from the chitinous oligosaccharides, βGlcNAc6-TSC and βGlcN6-TSC, was carried out by applying spontaneous chemisorption behavior of sugar S-derivatives to an Au substrate, as illustrated in Fig. 1, and investigated in detail by QCM and XPS analyses. QCM monitoring is able to elucidate the delicate adsorption behavior of sugar–TSCs on the Au surface of the QCM sensor chip. Fig. 2 shows frequency variation profiles as a function of time after stepwise injections of TSC-modified and TSC-free carbohydrates. The arrows indicate repeated injections of each sample. In the case of βGlcNAc6-TSC (Fig. 2a) and βGlcN6-TSC (Fig. 2b), the QCM frequency immediately dropped after the first injection at pH 4.0, and gradually decreased with subsequent sample injections. By contrast, neither TSC-free βGlcNAc6 nor TSC-free βGlcN6 were chemisorbed onto the Au surfaces since negligible frequency changes were observed. These results strongly indicated that both carbohydrate–TSCs interacted with the Au surface of the QCM sensor chips through a σ–π coordinate bond acting between S and Au atoms (Ning, Xie, Xing, Deng, & Yang, 1996).

However, it was found that larger amounts of both βGlcN6-TSC and TSC-free βGlcN6 were adsorbed on the Au surfaces at neutral pH 7.0 (Fig. 2d), although there was nearly no difference in the adsorption of βGlcNAc6 with or without TSC (Fig. 2c). There-

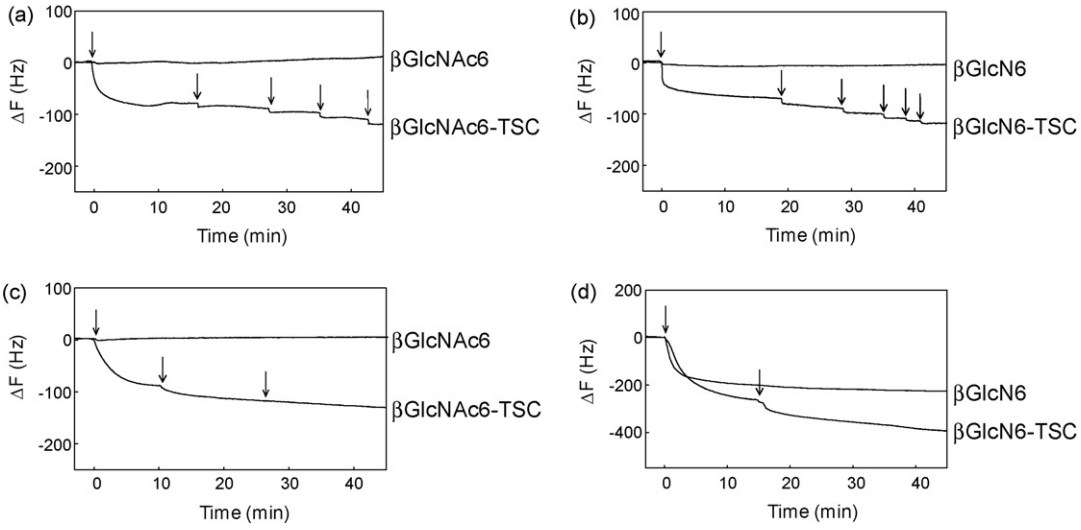

Fig. 2. QCM profiles of (a and c) βGlcNAc6 and (b and d) βGlcN6, with or without TSC-labeling. (a and b) pH 4.0 and (c and d) pH 7.0 of the analyte solution in the QCM sample chamber.

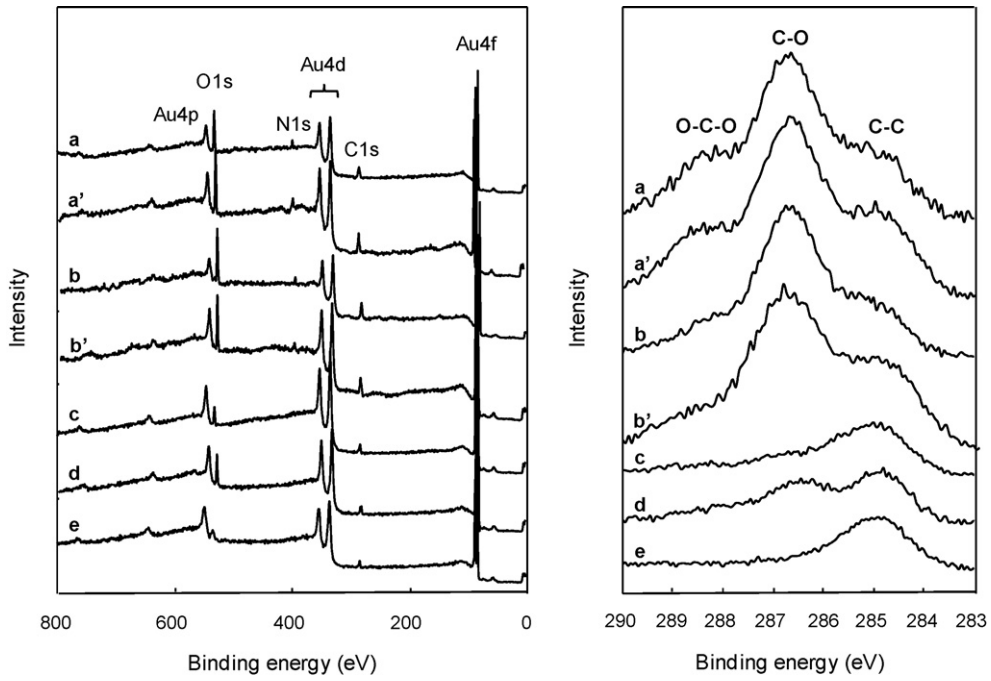

Fig. 3. XPS spectra of (left) survey and (right) C 1s narrow regions of carbohydrate-SAMs. (a and a′) βGlcNAc6-SAM, (b and b′) βGlcN6-SAM, (c) TSC-free βGlcNAc6, (d) TSC-free βGlcN6, and (e) basal Au substrate: (a′ and b′) after the sterilization *via* UV irradiation.

fore, additional interaction between Au and NH_2, as reported by Huang and Yang (2004), possibly occurred at neutral pHs. Simple pH control of carbohydrate–TSC solutions, however, could avoid such undesirable chemisorption due to the protonation of GlcN6 species from NH_2 to NH_3^+. The approximate sugar densities of βGlcNAc6-SAM and βGlcN6-SAM on the Au surfaces were estimated from the plateau frequency after several injections at pH 4.0 to be 0.39 and 0.35 chains nm^{-2}, respectively. These QCM results strongly suggest that βGlcNAc6-TSC and βGlcN6-TSC molecules were densely chemisorbed onto the Au surfaces where oligosaccharide chains were oriented to some extent from the bottom plate to the surface *via* terminal fixation of their reducing ends.

XPS analysis was performed to determine the elemental composition and chemical states of the surfaces of the carbohydrate-SAMs, as shown in Fig. 3. Survey scan spectra of βGlcNAc6-SAM and βGlcN6-SAM displayed clear C 1s, N 1s, O 1s and Au-related photoelectron peaks. In particular, characteristic N 1s peaks originating from *N*-acetylamino groups of GlcNAc and amino groups of GlcN were detected only on the sugar-SAM surfaces: no N 1s peak was found in other control samples, bare Au plate and the Au substrates treated with TSC-free carbohydrates. In addition, the C 1s narrow-scan spectra of βGlcNAc6-SAM and βGlcN6-SAM exhibited characteristic C–C/C–H (285.0 eV), possible C–N (*ca.* 285.9 eV, not clearly detected), C–O (*ca.* 286.7 eV) and O–C–O/C=O (*ca.* 288.1 eV) signals. In the case of other control samples, only a weak C–C peak was detected at 285.0 eV, consistent with the presence of hydrocarbon contaminants (Kohiki & Oki, 1984). There was almost no change found in the XPS profiles after the sterilization *via* UV irradiation. These results suggested successful formation of stable βGlcNAc6-SAM and βGlcN6-SAM on Au plates from corresponding TSC-derivatives, while TSC-free carbohydrates were mostly removed by washing post-treatment. Moreover, the strong Au peaks indicate that both carbohydrate-SAMs were very thin (<10 nm) due to the depth detection limit for XPS measurement (Kurzer & Douraghi-Zadeh, 1967). This finding is reasonable since the extended lengths of βGlcNAc6 and βGlcN6 chains are only *ca.* 3 nm. QCM and XPS results revealed that self-assembly chain immobilization of βGlcNAc6-TSC and βGlcN6-TSC was achieved on the Au surfaces *via* specific S–Au bonding.

3.2. Surface morphology and wettability of βGlcNAc6- and βGlcN6-SAMs

Surface morphology and roughness of chitinous SAMs were evaluated by tapping mode AFM imaging. As illustrated in Fig. 4, the Au-coated glass surface appeared to be composed of many nano-colloids, possibly due to Au nano-deposits, and was very flat at the nanometer scale: the root mean square (RMS) roughness was 1.14 ± 0.04 nm. In the cases of βGlcNAc6-SAM and βGlcN6-SAM, the surface roughness became slightly greater than for carbohydrate-free Au plate, with RMS values 1.38 ± 0.05 and 1.71 ± 0.16 nm, respectively, but these surfaces were nonetheless very smooth. These results suggested that the original morphology of basal Au substrate was maintained to some extent after the surface treatment with βGlcNAc6-TSC and βGlcN6-TSC. The maximum extended molecular lengths of βGlcNAc6 and βGlcN6 used in this study were *ca.* 3 nm, and thus both carbohydrate–TSCs were possibly chemisorbed on the Au surfaces through S–Au bonding to form 3 nm monolayers. This approach would enable preparation of βGlcNAc6-SAM and βGlcN6-SAM with designed shapes reflecting the basal surface morphology.

The surface wettability of scaffold substrates has a great influence on cell attachment, and in general adequate hydrophobicity

Table 1
Contact angles of a water droplet on each substrate.

Substrate	Contact angle (°)
Au plate	69.5 ± 1.7
βGlcNAc6-SAM	11.9 ± 2.0
βGlcN6-SAM	13.2 ± 4.2
βGlcNAc6[a]	30.6 ± 1.8
βGlcN6[a]	40.6 ± 2.7

[a] Au-coated plate was soaked in a 0.1% (w/v) aqueous solution of each TSC-free carbohydrate at R.T. for 24 h, followed by washing with Milli-Q water and ethanol.

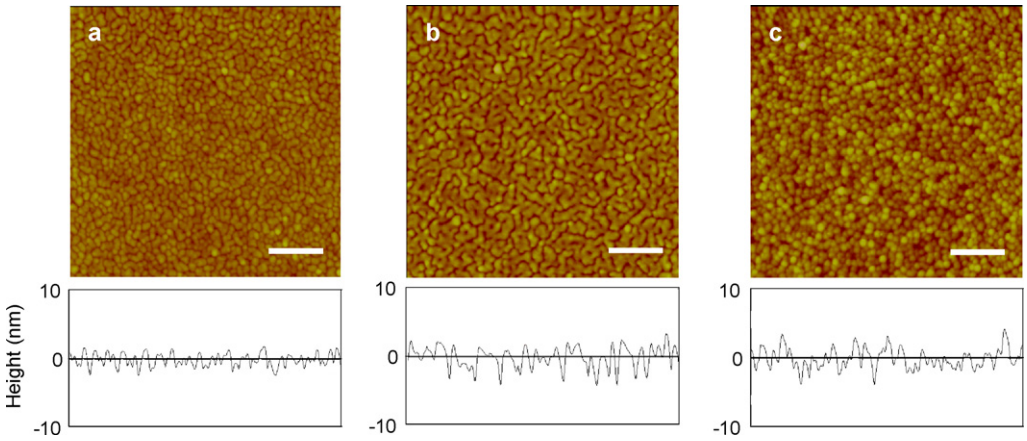

Fig. 4. AFM images of (a) basal Au substrate, (b) βGlcNAc6-SAM and (c) βGlcN6-SAM. The scale bars correspond to 0.2 μm.

is required in practice (Maroudas, 1975). Table 1 lists the contact angle values for water on βGlcNAc6-SAM, βGlcN6-SAM, intact Au plate and Au plates treated with TSC-free βGlcNAc6 or with TSC-free βGlcN6. The water contact angle of the Au plate was *ca.* 69.5°, showing relatively low wettability due to the hydrophobicity of Au metal. By contrast, βGlcNAc6-SAM and βGlcN6-SAM exhibited drastic decreases in water contact angle, as compared to Au plates treated with TSC-free carbohydrates. QCM (Fig. 2) and XPS (Fig. 3) data supported the presence of sugar molecules on the Au plates only through the TSC anchor, thus the hydrophilicity of the βGlcNAc6-SAM and βGlcN6-SAM surfaces was associated with the fixed chitinous oligomers. Furthermore, both sugar densities reached 0.3–0.4 chains nm^{-2}, hence it was presumed that the non-reducing ends of βGlcNAc6 and βGlcN6 were densely exposed to the outer surfaces. Conventional immobilization, *e.g.* spin-coating of polysaccharides, cannot control the molecular orientation, whereas TSC-mediated fixation enabled parallel chain immobilization, resulting in the formation of hydrophilic, accumulated sugar non-reducing ends, which play significant roles in various biological phenomena (Shimamura, 2008; Yamasaki, Nasholds, Schneider, & Apicella, 1991). The fabrication of nano-flat, hydrophilic, and stable carbohydrate-SAMs from water-soluble βGlcNAc6-TSC and βGlcN6-TSC was successfully achieved. Cell culture assay of the as-prepared SAMs is discussed in the following section.

3.3. *Cell adhesion and proliferation behavior on βGlcNAc6- and βGlcN6-SAMs*

Chitin and chitosan are inherently biocompatible, hence these SAMs were expected to be applicable as bio-functional materials. Simple bio-assay using mouse fibroblast NIH-3T3 cells was carried out to investigate the effects of βGlcNAc6-SAM and βGlcN6-SAM on cell adhesion and growth. Fig. 5 compares the initial and long-term cell adhesion behavior on the substrates βGlcNAc6-SAM, βGlcN6-SAM, intact Au plate and TCPS plate. The carbohydrate-SAMs prepared were transparent (light blue, Fig. 1), thus continuous monitoring of cell behavior was possible. Fig. 6 displays microscopic images of NIH-3T3 cells cultured on each substrate. It is apparent that NIH-3T3 cells adhered preferentially to both βGlcNAc6-SAM and βGlcN6-SAM, and fewer cells were attached to the more hydrophobic, sugar-free Au plate. Most of the cells on the βGlcNAc6-SAM and βGlcN6-SAM surfaces possessed flat morphology, indicating good cell attachment, and likewise on the commercial TCPS plate. In long-term incubation NIH-3T3 cells on the chitinous surfaces proliferated well to eventually almost reach confluence. Microscopic monitoring revealed good proliferation and extension of attached cells. On the other hand, some aggregation of seeded cells was observed on the sugar-free Au surface. Similar inefficiency was found for Au plates treated with TSC-free carbohydrates; a lot of floating or aggregated cells were observed. Commercial TCPS exhibited better cell adhesion performance than sugar-SAMs; however, these substrates had very different surface properties. It is well known that adherent cells have affinity for moderately hydrophobic substrates since cell adhesion occurs *via* serum proteins pre-adsorbed to the substrate surfaces through hydrophobic interaction (Nakanishi et al., 2006). The water contact angle value of TCPS plate ($53.9 \pm 2.1°$) was suitable for such cell adhesion. By contrast, βGlcNAc6-SAM and βGlcN6-SAM were very hydrophilic (with contact angles 12–13°), which were disadvantageous for general cell attachment. However, both carbohydrate-SAMs demonstrated good initial cell adhesion, and βGlcNAc6-SAM in particular showed excellent adhesion performance that was equivalent to that of TCPS plate. These results possibly indicate that the molecular function and orientation of βGlcNAc6 and βGlcN6 were closely involved in the initial cell adhesion behavior of NIH-3T3 cells.

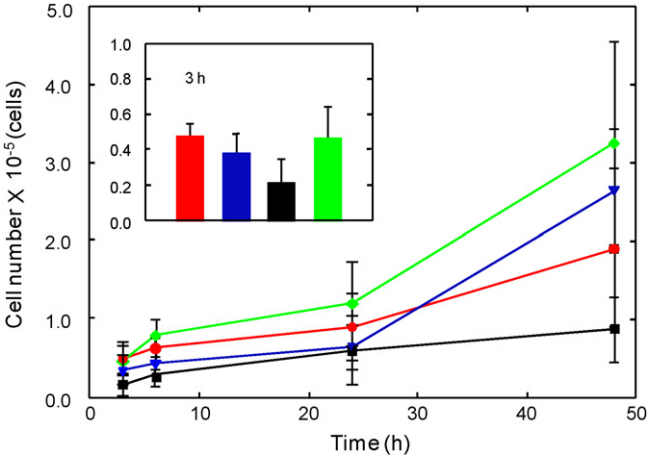

Fig. 5. Cell adhesion behavior on each substrate after 3, 6, 24 and 48 h. βGlcNAc6-SAM (red circles and bar), βGlcN6-SAM (blue triangles and bar), Au plate (black square and bar), and TCPS (green diamonds and bar). The inset vertical bar graph shows the initial cell attachment after 3 h incubation. (For interpretation of the references to color in this figure legend, the reader is referred to the web version of the article.)

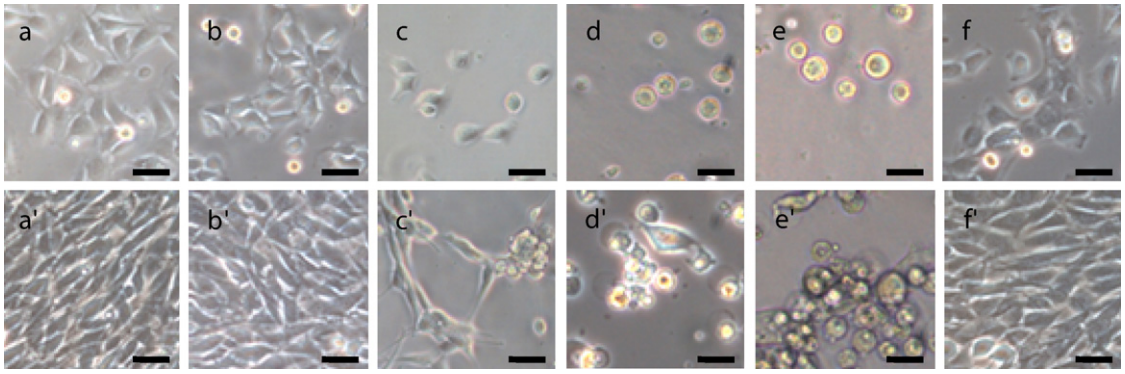

Fig. 6. Microscopic images of NIH-3T3 cell proliferation on (a and a′) βGlcNAc6-SAM, (b and b′) βGlcN6-SAM, (c and c′) sugar-free Au plate, (d and d′) TSC-free βGlcNAc6-treated Au plate, (e and e′) TSC-free βGlcN6-treated Au plate and (f and f′) TCPS after (a–f) 3 h and (a′–f′) 48 h incubation. The scale bars correspond to 100 μm.

The additional advantage of the βGlcNAc6-SAM and βGlcN6-SAM was shown in long-term incubation. Within 48 h after cell seeding, NIH-3T3 cells on the Au plate aggregated and could not proliferate; thus the Au plate had no biocompatibility for the NIH-3T3 cells. By contrast, both βGlcNAc6-SAM and βGlcN6-SAM maintained their original biocompatibility during 48 h incubation, and βGlcN6-SAM, particularly, demonstrated growth-promoting activity. A possible implication is that the amino groups of chitosan oligomers might make a preferential contribution to better proliferation of NIH-3T3 cells. In general, bioactive oligosaccharides are soluble in water, and thus frequently difficult to use in aqueous cell culture media. Thus, the strong point of these SAMs was to create the layer-state chitin and chitosan oligosaccharides whose inherent biocompatibility and growth-promoting activity were maintained for long periods in aqueous media. Chemoselective modification of the reducing ends of chitin and chitosan oligomers was effective for forming the glyco-scaffolds without significantly affecting their molecular functions. The cell culture assay results strongly suggest that hydrophilic βGlcNAc6-SAM and βGlcN6-SAM possessed excellent cell adhesion activity. This method is applicable to other carbohydrates, and thus further functional design will become possible.

4. Conclusion

The chitinous hexaoligosaccharides, βGlcNAc6 and βGlcN6, were successfully self-assembled on a transparent Au substrate through site-selective labeling of the sugar reducing ends with TSC. The resulting βGlcNAc6-SAM and βGlcN6-SAM possessed nanoscale flatness, hydrophilic properties, and exhibited good cell adhesion/proliferation behavior for initial and long-term culture. NIH-3T3 cells preferentially adhered to both βGlcNAc6-SAM and βGlcN6-SAM within 3 h of cell seeding, while fewer cells were attached to basal Au plate. This approach enables water-soluble oligosaccharides to be covalently immobilized on nano-flat surfaces, and as-designed SAMs demonstrate good biocompatibility even after long-term incubation in an aqueous cell culture medium. Such architectural design of carbohydrate-SAMs *via* self-assembly sugar-chain immobilization is expected to provide a new approach for the functional development of carbohydrate-decorated biointerfaces.

Acknowledgments

This research was supported by a Research Fellowship for Young Scientists from the Japan Society for the Promotion of Science (S.Y.) and by a Grant-in-Aid for Young Scientists (S: 21678002) from the Ministry of Education, Culture, Sports, Science and Technology, Japan (T.K.).

References

Barbucci, R., Magnani, A., Chiumiento, A., Pasqui, D., Cangioli, I., & Lamponi, S. (2005). Fibroblast cell behavior on bound and adsorbed fibronectin onto hyaluronan and sulfated hyaluronan substrates. *Biomacromolecules*, *6*, 638–645.

Boyan, B. D., Hummert, T. W., Dean, D. D., & Schwartz, Z. (1996). Role of material surfaces in regulating bone and cartilage cell response. *Biomaterials*, *17*, 137–146.

Chen, L., Du, Y., Wu, H., & Xiao, L. (2002). Relationship between molecular structure and moisture-retention ability of carboxymethyl chitin and chitosan. *Journal of Applied Polymer Science*, *83*, 1233–1241.

Huang, H., & Yang, X. (2004). Synthesis of chitosan-stabilized gold nanoparticles in the absence/presence of tripolyphosphate. *Biomacromolecules*, *5*, 2340–2346.

Kohiki, S., & Oki, K. (1984). Problems of adventitious carbon as an energy reference. *Journal of Electron Spectroscopy and Related Phenomena*, *33*, 375–380.

Kurzer, F., & Douraghi-Zadeh, K. (1967). Advances in the chemistry of carbodiimides. *Chemical Reviews*, *67*, 107–152.

Ligler, S. F., Lingertfelt, M. B., Price, R. P., & Schoen, P. E. (2001). Development of uniform chitosan thin-film layers on silicon chips. *Langmuir*, *17*, 5082–5084.

Lim, J. Y., Liu, X., Vogler, E. A., & Donahue, H. J. (2004). Systematic variation in osteoblast adhesion and phenotype with substratum surface characteristics. *Journal of Biomedical Materials Research A*, *68*, 504–512.

Maroudas, N. G. (1975). Polymer exclusion, cell adhesion and membrane fusion. *Nature*, *254*, 695–696.

Mori, T., Sekine, Y., Hasegawa, M., & Okahata, Y. (2007). Nanometer-scale immobilization of polysaccharides on hydrophobic polymer plates in supercritical fluoroform/water emulsions. *Biomacromolecules*, *8*, 2815–2820.

Morimoto, M., Saimoto, H., & Shigemasa, Y. (2002). Control of functions of chitin and chitosan by chemical modification. *Trends in Glycoscience and Glycotechnology*, *78*, 205–222.

Nakanishi, J., Kikuchi, Y., Takarada, T., Nakayama, H., Yamaguchi, K., & Maeda, M. (2006). Spatiotemporal control of cell adhesion on a self-assembled monolayer having a protecting group. *Analytica Chimica Acta*, *578*, 100–104.

Ning, Y., Xie, H., Xing, H., Deng, W., & Yang, D. (1996). Comparison of self-assembled monolayers of *n*-alkanethiols and phenylthioureas on the surface of gold. *Surface and Interface Analysis*, *24*, 667–670.

Ogushi, Y., Sakai, S., & Kawakami, K. (2009). Phenolic hydroxy groups incorporated for the peroxidase-catalyzed gelation of a carboxymethylcellulose support: cellular adhesion and proliferation. *Macromolecular Bioscience*, *9*, 262–267.

Onodera, T., Niikura, K., Iwasaki, N., Nagahori, N., Shimaoka, H., Kamitani, R., et al. (2006). Specific cell behavior of human fibroblast onto carbohydrate surface detected by glycoblotting films. *Biomacromolecules*, *7*, 2949–2955.

Park, I.-K., Yang, J., Jeong, H.-J., Born, H.-S., Harada, I., Akaike, T., et al. (2003). Galactosylated chitosan as a synthetic extracellular matrix for hepatocytes attachment. *Biomaterials*, *24*, 2331–2337.

Pasqui, D., Atrei, A., & Barbucci, R. (2007). A novel strategy to obtain a hyaluronan monolayer on solid substrates. *Biomacromolecules*, *8*, 3531–3539.

Rinaudo, M. (2006). Chitin and chitosan: properties and applications. *Progress in Polymer Science*, *31*, 603–632.

Shimamura, M. (2008). Non-reducing end α-mannosylated glycolipids as potent activators for invariant Vα19 TCR-bearing natural killer T cells. *Carbohydrate Research*, *343*, 2010–2017.

Suzuki, D., Takahashi, M., Abe, M., Sarukawa, J., Tamura, H., Tokura, S., et al. (2008). Comparison of various mixtures of β-chitin and chitosan as a scaffold for three-dimensional culture of rabbit chondrocytes. *Journal of Materials Science: Materials in Medicine*, *19*, 1307–1315.

Tamura, H., Nagahama, H., & Tokura, S. (2006). Preparation of chitin hydrogel under mild conditions. *Cellulose*, *13*, 357–364.

Xu, J., Mccarthy, S. P., & Gross, R. A. (1996). Chitosan film acylation and effects on biodegradability. *Macromolecules*, *29*, 3436–3440.

Yamasaki, R., Nasholds, W., Schneider, H., & Apicella, M. A. (1991). Epitope expression and partial structural characterization of F62 lipooligosaccharide (Los) of *Neisseria gonorrhoeae*: IgM monoclonal antibodies (3F11 and 1-1-M) recognize non-reducing termini of the los components. *Molecular Immunology*, *28*, 1233–1242.

Yokota, S., Kitaoka, T., Opietnik, M., Rosenau, T., & Wariishi, H. (2008). Synthesis of gold nanoparticles for in situ conjugation with structural carbohydrates. *Angewandte Chemie International Edition*, *47*, 9866–9869.

Yokota, S., Kitaoka, T., Sugiyama, J., & Wariishi, H. (2007). Cellulose I nanolayers designed by self-assembly of its thiosemicarbazone on a gold substrate. *Advanced Materials*, *19*, 3368–3370.

Yokota, S., Kitaoka, T., & Wariishi, H. (2008). Biofunctionality of self-assembled nanolayers composed of cellulosic polymers. *Carbohydrate Polymers*, *74*, 666–672.

Yokota, S., Matsuyama, K., Kitaoka, T., & Wariishi, H. (2007). Thermally responsive wettability of self-assembled methylcellulose nanolayers. *Applied Surface Science*, *253*, 5149–5154.